Iraqi Journal of Biotechnology

Iraqi Journal of Biotechnology, 2026, Vol. 25, No. 1, 228-246.

Enhancing the Stability and Efficiency of protease and lipase Immobilization in Magnetic Iron Oxide Nanoparticles coated with acacia gum

[1]Murtadha Aabdulhasan Aldhalemi, [2] Azhar Jawad Shanshool , [3] Ali A Taha

[1] University of Baghdad Department of Food Science, [2]University of Baghdad Department of Food Science

[3]University of Technology, Baghdad, Applied sciences department

Received: October 20, 2024 / Accepted: October 23, 2024 / Published: March 30, 2026

Abstract

Background. Immobilizing enzymes onto magnetic iron oxide nanoparticles provides a robust alternative to traditional methods, addressing challenges like high enzyme costs and environmental sensitivity. These three-dimensional matrices offer superior structural stability, extended storage longevity, and easy magnetic separation from reaction solutions. **Aim.** This study aims to characterize and utilize gum arabic-coated magnetic iron oxide nanoparticles for the efficient immobilization of protease and lipase enzymes. **Methods**. Nanoparticles were characterized using FE-SEM, AFM, FTIR, and XRD, both before and after coating with gum arabic (0.05 mg/L). The coated nanoparticles were then activated with glutaraldehyde. Subsequently, 10 mL of enzyme solutions were added in a 2:1 ratio to 0.5 mg of the activated support matrices to facilitate immobilization. The effects of time intervals, enzyme weight, pH, and temperature on the process were systematically evaluated. **Results**. Advanced characterization successfully confirmed both the gum arabic encapsulation and the subsequent enzyme immobilization. The experimental immobilization efficiencies ranged broadly from 25% to 80%. Notably, the process resulted in exceptional activity recoveries, reaching up to 120% for protease and 130% for lipase. Furthermore, the data showed that enzyme weight, pH variations (4 to 8), and temperature ranges (30 to 50 °C) significantly influenced both the immobilization efficiency and the final recovery of enzyme activity. **Conclusion.** Magnetic iron oxide nanoparticles serve as highly effective support matrices for enzyme immobilization. This approach successfully enhances enzyme stability, activity, and reusability, offering a highly viable solution to critical challenges in biochemical applications

Keywords: Iron oxide nanoparticles, lipase enzyme, protease enzyme, immobilization efficiency, gum arabic, glutaraldehyde.

Corresponding author: Azhar.j@coagri.uobaghdad.edu.iq

Introduction

Protease and lipase enzymes are crucial for various biological processes, particularly in the degradation of proteins and fats. Immobilizing these enzymes on magnetic iron oxide nanoparticles is a promising research avenue. These nanoparticles not only provide a large surface area and favorable chemical interactions for enzyme attachment but also enhance enzyme stability, preventing degradation. Additionally, immobilization allows for better control over the release and separation of enzymes from reaction mixtures, facilitating their reusability and efficiency in

biocatalytic applications. (1). Studies have demonstrated that the use of these materials can enhance immobilization efficiency and increase enzyme stability under various conditions. Multiple factors, such as temperature, enzyme quantity, pH, and immobilization time, can significantly influence the efficiency of immobilization and the recovery rate of enzyme activity (2).

Research indicates that variations in temperature can have a substantial impact on enzyme activity. For instance, studies have shown that increasing temperature can enhance enzyme activity up to a certain point, after which activity begins to decline due to the denaturation of the enzyme's protein structure (3). Conversely, changes in pH can affect the electric charges on the enzyme's surface, thereby influencing the immobilization interactions. Furthermore, the amount of enzyme used in the experiment plays a critical role in immobilization efficiency (4). Studies have indicated that increasing the enzyme quantity leads to a rise in immobilization percentage until a saturation point is reached, beyond which no additional increase in activity occurs (5). Additionally, immobilization time is an important factor; research has shown that extending the time leads to an increase in immobilization percentage until equilibrium is reached, at which point no significant change in activity is observed (6).

Therefore, the objective of this research is to investigate the potential of encapsulating nanoparticles and the feasibility of immobilizing enzymes onto them, while also examining the effects of various immobilization factors on the efficiency of immobilization and the recovery rate of enzyme activity (7).

Materials and methods

Materials

Protease and lipase enzymes were obtained from Solarbio (China), isolated from the mold Aspergillus niger.Magnetic iron oxide nanoparticles, with a size of 30 nm, were sourced from SkySpring Nanomaterials (USA). Acacia gum (Gum Arabic) was procured from Thomas Baker (India), and sodium hydroxide was obtained from Riedel-de Haën (Germany). Potassium phosphate dibasic and monobasic were acquired from CDH (India) and HIMEDIA (India), respectively. Olive oil was purchased from ZER (Turkey), while acetone and casein were sourced from BDH (England). Ethanol was procured from Cristalco (France), and Coomassie Blue G250 was obtained from the UK. Potassium bromide was sourced from AVONCHEM (UK). Additionally, Bovine Serum Albumin (BSA), tyrosine, and glutaraldehyde were acquired from DIREVO (Germany), and phosphoric acid was obtained from Riedel-de Haën (Germany). Trichloroacetic acid was procured from CDH (India).

Methods

Characterization of MNPs

Magnetic nanoparticles (MNPs) are characterized using a range of analytical tools to assess their physicochemical properties. The dimensions of nanoparticles significantly influence their various physicochemical characteristics, and even minor variations in their nanoscale size can lead to substantial changes in these properties. Among the instruments employed for the characterization of MNPs are Atomic Force Microscopy (AFM), Energy Dispersive X-ray Diffraction (EDXD), Field-Emission Scanning Electron Microscopy (FE-SEM), and Fourier Transform Infrared Spectroscopy (FT-IR) (8; 9;10;11;12; 13).

Surface Modification of MNPs with Gum Arabic (GA)

The surface of the Fe3O4 nanoparticles was coated with gum arabic through the process of mixing 0.5 g of the nanoparticles with 50 ml of a gum arabic solution at a concentration of 5 mg/L. The resulting mixture was subjected to sonication for a duration of 30 minutes at room temperature to ensure thorough dispersion and coating. Following sonication, the gum arabic-coated magnetic nanoparticles were separated from the reaction solution by placing a magnet beneath the container, which facilitated their recovery. The magnetic nanoparticles were then washed multiple times with distilled water to remove any unbound gum arabic. Finally, the loaded nanoparticles were dried in an oven at a temperature of 40°C for a period of 24 hours prior to their application in subsequent experiments (14).

Enzyme Immobilization:

Magnetic nano-iron oxides were loaded with gum arabic as per the established protocol. Subsequently, 0.25 g of the loaded particles was dispersed in 10 ml of a 5% glutaraldehyde solution (15; 16). Following this, 10 ml of a solution containing 0.09 g of protease and lipase enzymes, mixed in a ratio of 1:2, was prepared, and the enzyme activity was determined according to the specified method (17).

Activity Assay of Enzymes

Lipase activity was estimated according to the method mentioned by (18;19).and protease enzyme activity was estimated based on the method mentioned by (20).

Activity recovery and Specific activity were calculated using the following equations (21)

Specific activity (U/g protein) = initial activity / protein content of immobilized enzyme.

Activity recovery (%) = (activity of immobilized enzyme /total activity of free enzyme) × 100

Results

Characterization of Magnetic Nano-particles

1. Determination of the Shape and Size of Magnetic Iron Oxide Nanoparticles Using Scanning Electron Microscopy

Scanning electron microscopy (SEM) analysis revealed that the magnetic iron oxide nanoparticles exhibit a homogeneous, spherical morphology (Figure 1). The micrographs demonstrated a highly porous surface structure, alongside visible agglomeration of the nanoparticles into larger clusters. Furthermore, dimensional analysis confirmed an average particle size of 35 nm.

Scanning electron microscopy (SEM) analysis at a 50 nm scale revealed distinct morphological and dimensional changes in the magnetic iron oxide nanoparticles following their coating with gum arabic (GA) **(Figure 2)**. The micrographs demonstrated that the uncoated Fe3O4 nanoparticles possessed a spherical shape characterized by a rough surface and significant particle agglomeration. In contrast, the GA-coated nanoparticles (GA@MNPs) exhibited a noticeable increase in their average diameter, a smoother surface morphology, and a marked reduction in agglomeration compared to the uncoated particles.

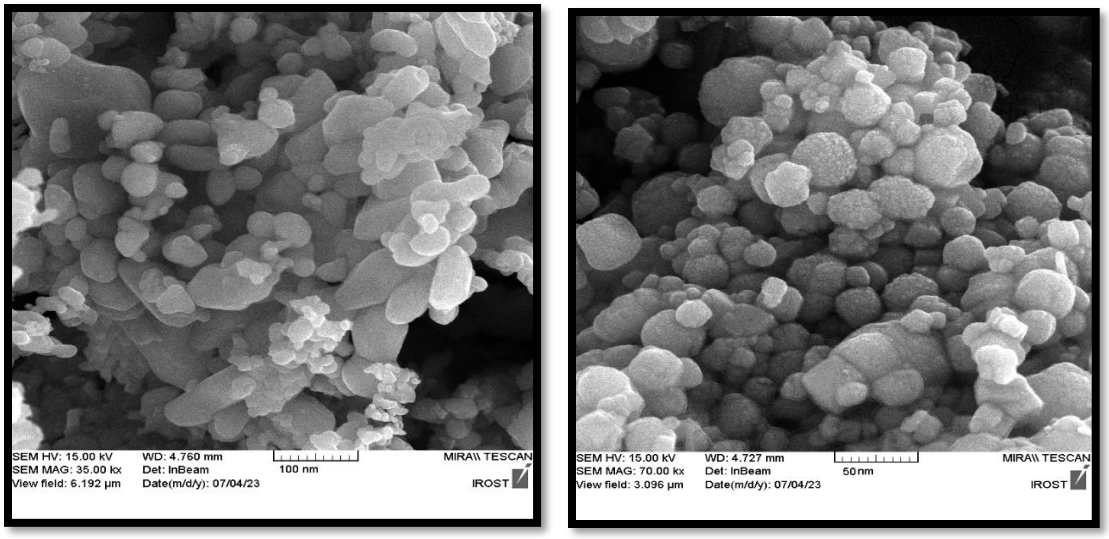

Figure (1) Shape and Size of Magnetic Iron Oxide Nanoparticles (MNPs) Using Field-Emission Scanning Electron Microscopy (FE-SEM).

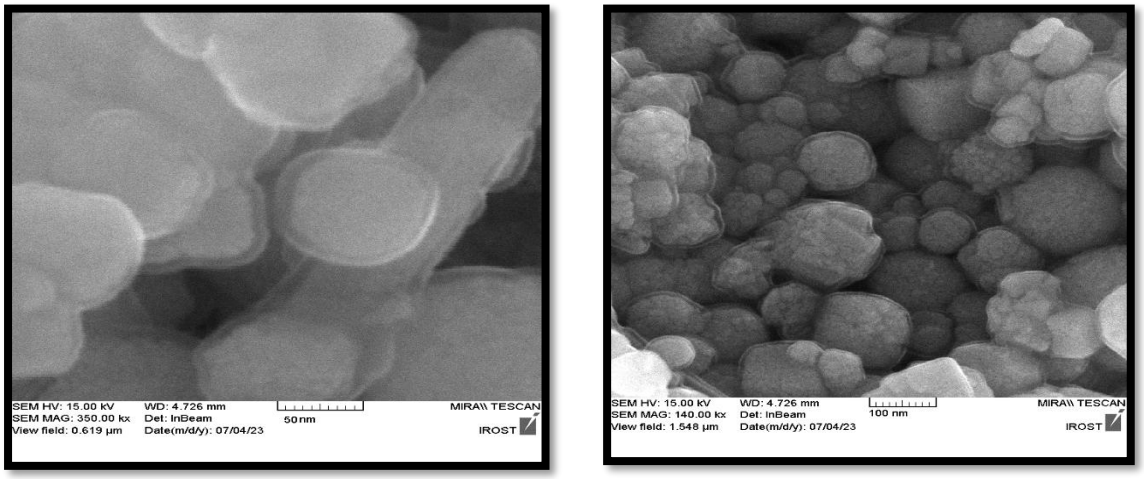

Figure (2) Shape and Size of Gum Arabic Loaded Magnetic Iron Oxide Nanoparticles (GA@MNP) Using Field-Emission Scanning Electron Microscopy (FE-SEM).

Scanning electron microscopy (SEM) analysis of the gum arabic-coated magnetic nanoparticles following the immobilization of protease and lipase enzymes (GA@MNP@Enzyme) revealed distinct morphological alterations **(Figure 3)**. The micrographs demonstrated that the surface of the enzyme-immobilized nanoparticles was more homogeneous compared to the bare nanoparticles and those coated solely with gum arabic. Additionally, the analysis indicated the presence of particle aggregates of varying sizes across the sample.

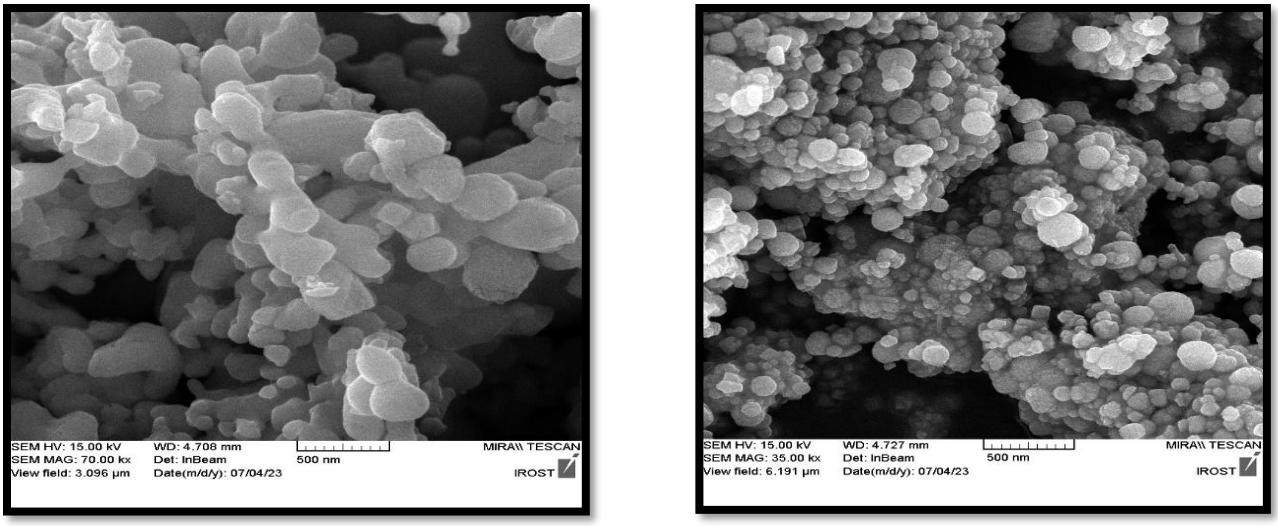

Figure (3) Shape and Size of Gum Arabic Loaded Magnetic Iron Oxide Nanoparticles After Enzyme Immobilization (GA@MNP@Enzyme) Using Field-Emission Scanning Electron Microscopy (FE-SEM).

2- Determining the shape of magnetic iron ox ide nanoparticles before and after coating with gum arabic using atomic force microscopy.

Atomic Force Microscopy (AFM) was employed to analyze the surface topography of the uncoated magnetic iron oxide nanoparticles. As depicted in the two-dimensional micrographs (Figure 4), the sample exhibited a homogeneous surface characterized by a uniform distribution of predominantly spherical particles. Furthermore, the corresponding three-dimensional topographical images revealed an interwoven structural arrangement of the nanoparticles. Quantitative analysis of the surface profile indicated that the average height of the particles was approximately 10 nm.

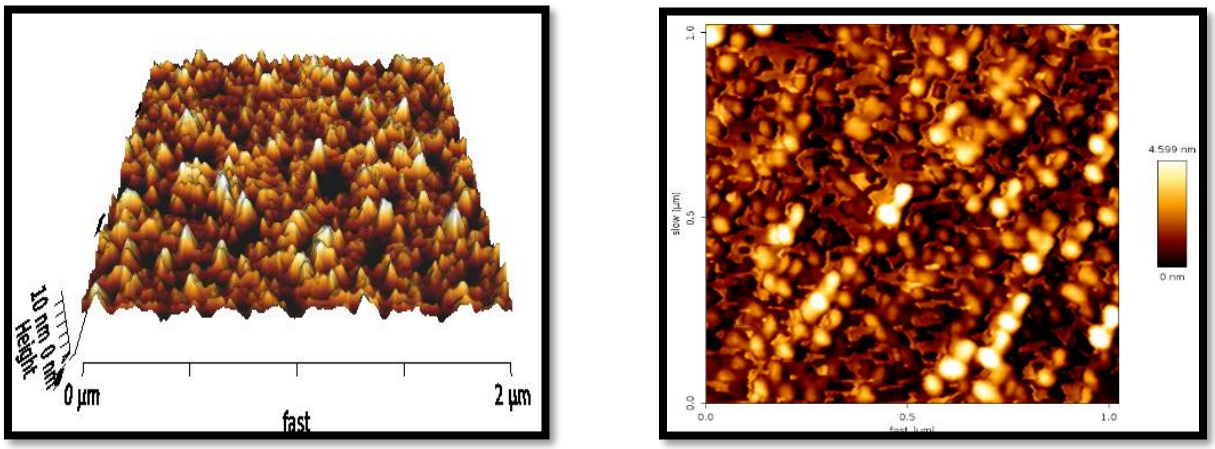

Figure (4) shows the morphology of magnetic iron oxide nanoparticles before being loaded with gum arabic, as observed using Atomic Force Microscopy (two-dimensional and three-dimensional images).

Atomic Force Microscopy (AFM) analysis of the gum arabic-coated magnetic nanoparticles (GA@MNPs) revealed distinct topographical features in both two-dimensional and three-dimensional micrographs (Figure 5). The two-dimensional images displayed a highly homogeneous surface characterized by the presence of distinct bright spots.

Furthermore, the corresponding three-dimensional images demonstrated a more interwoven structural arrangement compared to the uncoated nanoparticles (Figure 4). Quantitative topographical measurements indicated that the root mean square (RMS) surface roughness of the GA@MNPs was 1.11 nm, compared to an RMS value of 1.045 nm for the uncoated particles.

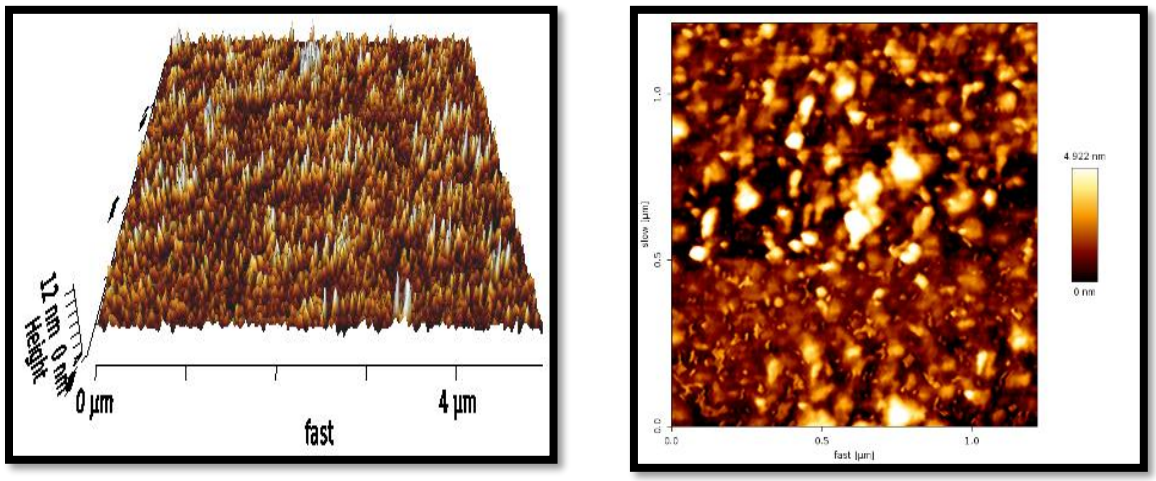

Figure (5) illustrates the magnetic iron oxide nanoparticles after being loaded with gum arabic, as observed using Atomic Force Microscopy (two-dimensional and three-dimensional images

Atomic Force Microscopy (AFM) was utilized to evaluate the topographical changes following the immobilization of the protease and lipase enzyme mixture onto the gum arabic-coated nanoparticles (GA@MNP@Enzyme). As illustrated in Figure 6, the AFM measurements demonstrated a significant increase in the surface height of the particles, measuring 30 nm for the GA@MNP@Enzyme sample, compared to 12 nm for the precursor GA@MNP particles.

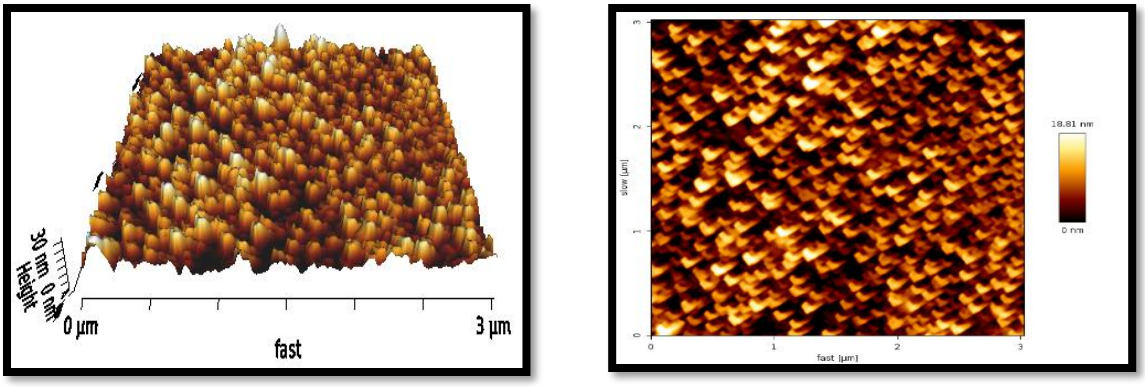

Figure (6) illustrates the magnetic iron oxide nanoparticles after being loaded with gum arabic and the immobilization of enzymes onto them, as observed using Atomic Force Microscopy (two-dimensional and three-dimensional images).

Atomic Force Microscopy (AFM) analysis revealed a significant increase in particle surface height following the immobilization of the enzyme mixture (Figure 6). Specifically, the surface height measured 12 nm for the precursor GA@MNP particles and increased to 30 nm for the resulting GA@MNP@Enzyme sample.

3- Identification of functional groups in magnetic nanoparticles before coating with gum arabic, after coating, and after enzyme immobilization using Fourier Transform Infrared Spectroscopy (FTIR).

The use of Fourier-transform infrared spectroscopy (FTIR) analysis is an appropriate method for identifying the functional groups present in organic compounds in the magnetic Fe3O4 nanoparticles sample. For this purpose, FTIR spectra of the nanoparticles were obtained using the KBr-Pellet method (28).

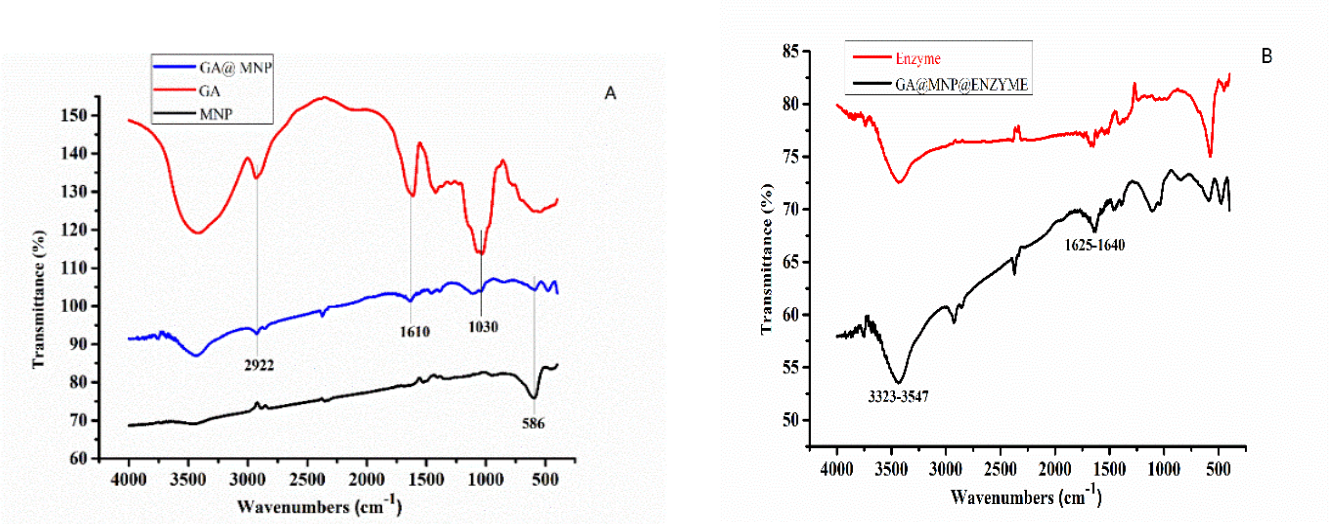

Figure (7-A, B) shows the infrared spectrum using Fourier-transform infrared spectroscopy (FTIR) for MNPs.

Fourier-transform infrared (FTIR) spectroscopy was performed within the 500–4000 cm^{-1} range to identify the functional groups of the samples. The FTIR spectrum of the uncoated magnetic nanoparticles (MNPs) (Figure 7) exhibited a broad absorption band between 490 and 594 cm^{-1}, with a prominent peak at 590 cm^{-1} corresponding to Fe-O stretching vibrations. The spectrum of pure gum arabic revealed a strong peak at 1610 cm^{-1} associated with the asymmetric stretching of C=O, and a band near 3417 cm^{-1} corresponding to O-H stretching vibrations. Additional absorption bands were recorded at 2922 cm^{-1} and 1030 cm^{-1}, assigned to C-H and carboxylate (COO) stretching vibrations, respectively.For the gum arabic-coated magnetic nanoparticles (GA@MNPs) (Figure A-7), the FTIR spectrum demonstrated broad bands at 590 cm^{-1} and 3437 cm^{-1}, attributed to Fe-O bonds and O-H stretching vibrations, respectively. Furthermore, distinct peaks corresponding to carboxyl groups were observed at 1104 cm^{-1} and 2216 cm^{-1}.Finally, the FTIR spectrum of the enzymes (Figure B-7) displayed absorption bands at 1640–1625 cm^{-1} and 3547–3323 cm^{-1}. These peaks correspond to the amide I (C=O stretching) and amide II (N-H stretching) bands, respectively.

4- Determination of the crystalline structure of magnetic iron oxide nanoparticles using X-ray diffraction.

X-ray diffraction (XRD) analysis was conducted to evaluate the crystalline structure of the samples. For the gum arabic-coated magnetic nanoparticles (GA@MNPs), the characteristic diffraction peaks of Fe_3O_4 were observed at the same 2θ values as the uncoated nanoparticles.

Specifically, diffraction peaks corresponding to the (220), (311), (400), (511), and (422) crystalline planes were identified. However, the intensity of these sharp crystalline peaks was reduced, accompanied by the appearance of broad peaks associated with the amorphous gum arabic. Following the immobilization of the enzymes onto the coated nanoparticles (GA@MNPs@ENZYME), the XRD pattern (Figure 8) demonstrated no significant shift in the positions of the crystalline peaks. Nevertheless, a further decrease in the overall peak intensity was recorded for the GA@MNPs@ENZYME sample compared to the precursor GA@MNPs.

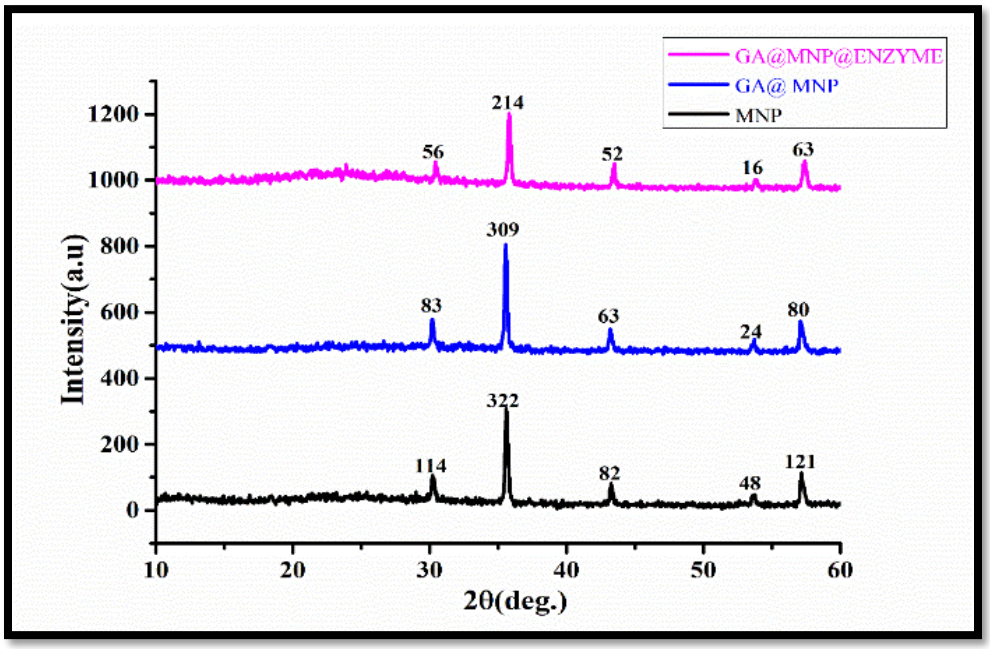

Figure (8): XRD analysis patterns for Fe_3O_4 MNPs, GA@MNPs, GA@MNPs@Enzyme.

Enzyme activity and immobilization efficiency Enzyme activity

The catalytic activity of both the free and immobilized enzymes was quantitatively evaluated based on their rates of fat and protein hydrolysis. The enzymes immobilized onto the gum arabic-coated magnetic nanoparticles (GA@MNPs@ENZYME) demonstrated a fat hydrolysis rate of 3494.6 units/mg and a protein hydrolysis rate of 2450.53 units/mg. In comparison, the hydrolysis rates for the free, non-immobilized enzymes were recorded at 2688 units/mg for fats and 2250.92 units/mg for proteins.

Effect of different immobilization conditions on immobilization efficiency and activity recovery

Studying the effect of different immobilization conditions on enzyme performance is crucial for enhancing enzyme activity in various applications.

The presence of stabilizing agents during immobilization enhances the specific activity, as optimal immobilization conditions lead to higher specific activities, indicating that the enzyme retains its functional conformation and activity (39).

1-**Effect of immobilization time**

The impact of immobilization time on both immobilization efficiency and enzyme activity recovery was evaluated **(Table 1)**. The results indicated a direct correlation between the duration of the immobilization process and the density of enzyme loading; extending the immobilization time resulted in an increased density of immobilized enzymes. However, as illustrated in **Figure 9**, prolonging the immobilization period negatively affected the percentage of activity recovery. Based on the documented data, the optimal immobilization time was determined to be 2.5 hours, which yielded a maximum immobilization efficiency of 70%. This duration allows sufficient time for the enzyme to interact with the support, thereby increasing the number of enzymes that become covalently bound to the gum arabic-loaded magnetic iron oxide nanoparticles (40).

Table (1) Effect of Time on the Immobilization Process.

immobilization efficiency (%)	activity recovery lipase (%)	activity recovery proteas (%)	temperature
25	45	50	**1**
45	50	70	1.5
65	90	90	2
70	130	108	2.5
80	110	120	3

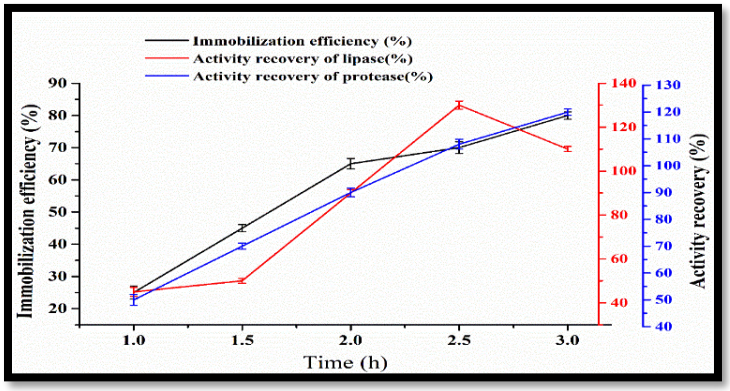

Figure (9) Effect of Immobilization Time on Immobilization Efficiency and Enzyme Activity Recovery.

At the optimal immobilization time, the maximum activity recovery (130.108%) was achieved for the protease and lipase enzymes, respectively (41). In his research, it was mentioned that extending the immobilization time increases activity recovery to a higher percentage. It is noted that extending the immobilization time leads to a decrease in the activity recovery of lipase, as shown in Figure (9).

Nevertheless, increasing the immobilization time results in higher immobilization efficiency for the target enzymes in this study on magnetic iron oxide nanoparticles.

2-Effect of immobilization temperature

The temperature of immobilization critically affects the efficiency and effectiveness of enzyme immobilization.

Table (2) Effect of Different Temperatures on Immobilization Efficiency, Specific Activity, and Activity Recovery

immobilization efficiency (%)	activity recovery lipase (%)	activity recovery proteas (%)	temperature
60	120	80	**30**
86	125	104	**35**
70	130	108	**40**
65	120	95	**45**
64	115	86	**50**

From Table (2), the effect of various temperatures on immobilization efficiency, specific activity, and activity recovery is observed, along with the study of improving the immobilization efficiency of enzymes on gum arabic-loaded magnetic nanoparticles. It is noted that the immobilization efficiency decreases with lower temperatures, as shown in Figure (10). While low temperatures can facilitate the immobilization of enzymes and reduce the degradation rate, they also decrease the rate of enzyme binding to the support due to the slowing of reaction kinetics (42).

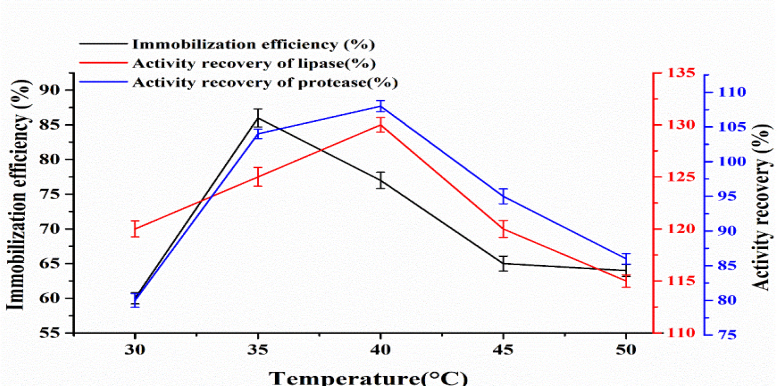

Figure (10) Effect of Different Temperatures on Immobilization Efficiency, Specific Activity, and Activity Recovery.

Figure (10) shows that each enzyme has an optimal temperature range that enhances its activity and stability. Reactions within this range during immobilization can promote enzyme binding and maintain activity, thereby reflecting an improvement in immobilization efficiency and specific activity. Enzyme immobilization was conducted over a temperature range of 30 to 50 degrees Celsius, where a continuous improvement in immobilization efficiency was observed.

Despite the increase in temperature, activity recovery significantly increased, peaking at 40 degrees Celsius with values of (108.130) % for lipase and protease enzymes, respectively. After this point, activity recovery began to decline due to the effects of high temperature on the enzymes, as shown in Figure (10). Based on these results, 40 degrees Celsius was determined to be the optimal temperature for immobilization (36;38).

These results can be interpreted as low temperatures enhancing enzyme properties, such as stability and conformation, which reduces protein degradation in the buffer solution, as mentioned by Kumar *et al*. (42). The decrease in immobilization capacity after the optimal temperature may be due to the enzymes gaining higher energy, leading to destructive collisions that result in enzyme degradation and affect enzyme immobilization on carrier matrices (27). In general, the rate of enzyme reaction increases with rising temperature up to a certain level, after which higher temperatures lead to protein degradation and thus a decrease in reaction rate. From this, we conclude that extreme temperatures (both low and high) can reduce immobilization efficiency and specific activity, either through insufficient binding or structural changes (40).

3- **Effect of pH value**

The pH value during the immobilization process is crucial for determining the performance of immobilized enzymes. Selecting a pH value that maximizes enzyme stability and binding interactions is essential for achieving optimal immobilization efficiency (43). Table (3) shows the effect of pH values on immobilization efficiency, specific activity, and activity recovery. These different values were also studied in Table (3) to improve the efficiency of enzyme immobilization on gum arabic-loaded magnetic nanoparticles. Table (3) indicates that immobilization efficiency decreases with decreasing pH, as illustrated in Figure (11). Although the enzymes were immobilized on the targeted nanoparticle supports in this study at low pH values, this reduces the rate of enzyme binding to the support. This leads to insufficient binding efficiency, resulting in a decrease in overall enzyme loading (44).

Table (3) Effect of Different pH Levels on Immobilization Efficiency, Specific Activity, and Activity Recovery.

immobilization efficiency (%)	activity recovery lipase (%)	activity recovery proteas (%)	pH
38	20	45	**4**
45	60	75	**5**
50	90	95	**6**
70	130	108	**7**
80	125	85	**8**
40	70	70	**9**

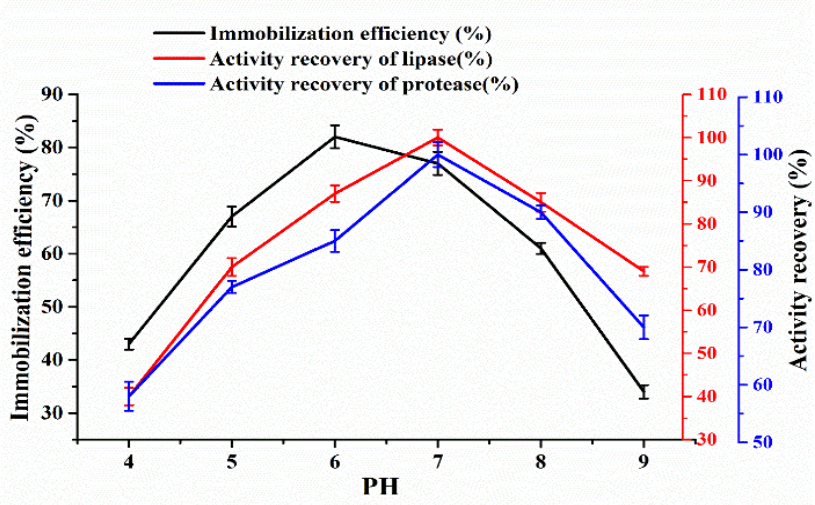

Figure (11) Effect of Different pH Levels on Immobilization Efficiency, Specific Activity, and Activity Recovery.

Despite the widespread use of glutaraldehyde for enzyme immobilization due to its ability to form stable covalent bonds with amino groups on the enzyme surface (27), the pH of the immobilization medium can significantly affect the availability of these amino groups and, consequently, the efficiency of immobilization. Figure (11) shows that as the pH increases to 9, both activity recovery and

protein loading of the enzyme on the magnetic nanoparticles significantly decrease, indicating that higher pH levels may hinder effective interactions between the enzyme and the nanoparticles (1;7). This suggests that maintaining a neutral to slightly alkaline pH during the immobilization process enhances the efficiency of enzyme binding to the magnetic nanoparticles. Furthermore, the concentration of glutaraldehyde used in the enzyme immobilization process plays an important role in the interaction with pH. Glutaraldehyde reacts with the amino groups in the enzyme, contributing to the formation of covalent bonds that lead to its immobilization on the support. As the pH changes, the charge of the functional groups in the enzyme also changes, affecting its interactions with glutaraldehyde. Additionally, pH can influence enzyme stability and, consequently, its efficiency in the reaction (4).

4-Effect of enzyme Amount

Table (4) illustrates that the effect of different enzyme amounts used during the immobilization process significantly impacts immobilization efficiency and activity recovery. It shows that increasing the enzyme quantity improves immobilization efficiency until the magnetic nanoparticles reach a saturation point, where all available binding sites on the support material are utilized (3). Table (4) also indicates that when large amounts are used, there may be a loss of unbound enzymes, which affects the overall efficiency of immobilization and activity recovery. Additionally, increasing enzyme quantities may lead to aggregation, reducing the binding effectiveness with the

nanoparticles and consequently decreasing the available surface area for interaction (16). High enzyme loading concentrations can lead to multilayer associations on the structure of gum arabic-loaded magnetic nanoparticles, reducing the surface area and also limiting the dispersed increase. While we hypothesized that high enzyme concentration results in a higher reaction rate from a reaction kinetics perspective, a similar increase in viscosity at high enzyme concentrations may reduce the mixing efficiency of the enzyme reaction mixture with the gum arabic-loaded magnetic iron oxide nanoparticles (6).

Table (4) Effect of Different Enzyme Amounts on Immobilization Efficiency, Specific Activity, and Activity Recovery.

Amount of Lipase (mg)	Number of proteas (mg)	Activity Recovery Lipase (%)	Activity Recovery proteas (%)	Immobilization Efficiency (%)
31	31	264	26	60
62	31	130	108	70
62	62	144	24	65
120	62	35	24	50
120	120	12	10	45
250	120	15	15	20

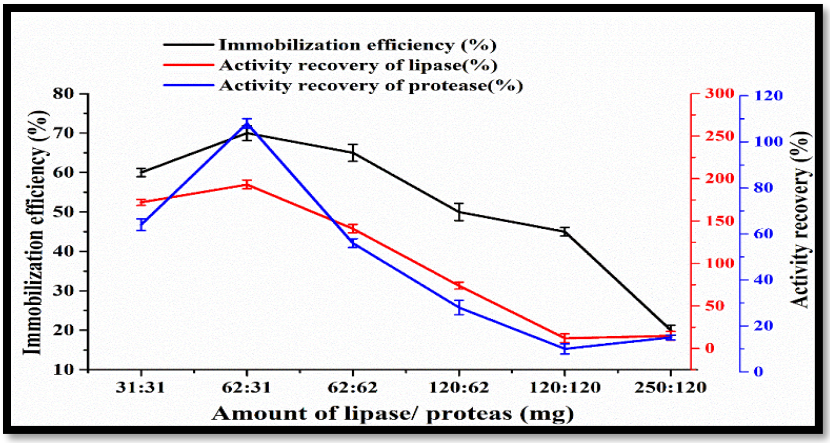

Figure (12) Effect of Different Enzyme Amounts on Immobilization Efficiency, Specific Activity, and Activity Recovery.

Figure (12) illustrates the balance between enzyme amount, immobilization efficiency, and high activity recovery percentage, with the highest immobilization efficiency (70%) achieved at enzyme amounts of 31 mg and 62 mg for lipase and protease, respectively. Therefore, it is important to consider the appropriate amount of enzyme to ensure optimal immobilization efficiency without negatively affecting activity. It appears that if the enzyme loading is high, the kinetic benefit of a higher enzyme concentration diminishes due to poor mass transfer efficiency, leading to decreased enzyme activity (45). Consequently, immobilization efficiency showed a consistent decline as loading increased; a large amount of enzyme loading can reduce activity recovery, as enzyme molecules hinder each other from accessing the substrate or being accessed by the substrate (44).

Discussion

1-Morphological and Structural Modifications

The morphological analysis revealed significant agglomeration in the uncoated Fe_3O_4 nanoparticles, a phenomenon primarily attributed to their inherently high surface energy, magnetic dipole-dipole interactions, and the effects of the sintering process (22, 23). The application of the gum arabic (GA) coating effectively mitigated this agglomeration, yielding a smoother and more homogeneous surface. This improvement is driven by the structural nature of GA; as a highly branched polysaccharide with hydrophilic properties, it provides excellent steric stabilization and prevents particle clustering (31, 32). The successful functionalization was corroborated by FTIR and AFM analyses, which showed increased surface height and distinct functional group interactions. Furthermore, the reduction in the intensity of sharp XRD peaks post-coating and post-immobilization confirms the successful incorporation of the amorphous GA polymer and the subsequent formation of an enzyme monolayer, which slightly masks the crystalline structure of the magnetic core without destroying its fundamental framework (24, 35).

2- Enhanced Catalytic Activity and Thermal Behavior

The immobilized lipase and protease exhibited superior hydrolytic activity compared to their free counterparts. This enhancement strongly suggests that the GA@MNPs support matrix provides a robust microenvironment that restricts the

conformational unfolding of the enzymes, thereby reducing steric hindrance and conferring higher structural stability (38, 39). Regarding thermal stability, while lower temperatures preserve the structural conformation and minimize protein degradation in the buffer solution, they inherently slow down the reaction kinetics and reduce the rate of enzyme binding to the support (42). Conversely, when temperatures exceed the optimal point (40 °C), the enzyme molecules acquire excessive kinetic energy. This leads to destructive collisions that disrupt the non-covalent interactions maintaining the enzyme's three-dimensional structure, ultimately resulting in thermal denaturation and a sharp decline in activity recovery (27, 40).

3- Optimization of Immobilization Parameters and Mass Transfer Limitations

The immobilization efficiency is strictly governed by the availability of binding sites and the efficiency of mass transfer. The use of glutaraldehyde facilitates stable covalent cross-linking between the support and the amino groups of the enzymes (27). However, this interaction is highly pH-dependent; extreme alkaline conditions alter the ionization state and charges of the functional groups, thereby hindering the cross-linking efficacy and reducing overall protein loading (1, 4, 7). Moreover, prolonged immobilization times and excessive enzyme concentrations proved counterproductive. High enzyme loading leads to nonspecific binding, aggregation, and the formation of multilayer associations on the nanoparticle surface. This aggregation not only increases the local viscosity—which impairs the mixing efficiency and mass transfer—but also causes severe steric hindrance, where densely packed enzyme molecules physically block one another from accessing the substrate molecules (3, 6, 16, 44, 45).

Conclusion

In this study, the successful coating of magnetic iron oxide nanoparticles and the immobilization of lipase and protease enzymes on gum arabic-loaded iron oxide nanoparticles were demonstrated. Additionally, the magnetic iron oxide nanoparticles were characterized using FE-SEM, AFM, XRD, and FT-IR techniques. FE-SEM showed that the magnetic iron oxide nanoparticles had an average size ranging from 30-35 nanometers, which increased to 40 nanometers after coating with gum arabic. After enzyme immobilization, the size reached approximately 150 nanometers. Meanwhile, AFM revealed changes in the morphological shape of the magnetic nanoparticles before coating, after coating, and after enzyme immobilization, along with variations in the average roughness (RMS) values: 1.045 nm before coating, 1.11 nm after coating, and 3.551 nm after enzyme immobilization. Furthermore, XRD indicated that the crystallinity of the magnetic nanoparticles was unaffected by the coating and immobilization processes. Changes in immobilization efficiency were observed with varying immobilization factors such as immobilization time, enzyme amount, temperature, and pH. The best results were achieved at an immobilization time of 2.5 hours and enzyme amounts of 31 mg and 62 mg for protease and lipase, respectively, at a temperature of 40°C and a pH of 7, with an immobilization efficiency of 70% and activity recovery percentages of (108.130) % for lipase and protease, respectively.

References

1. Hajareh Haghighi, F., Binaymotlagh, R., Palocci, C., & Chronopoulou, L. (2024). Magnetic Iron Oxide Nanomaterials for Lipase Immobilization: Promising Industrial Catalysts for Biodiesel Production. *Catalysts*, *14*(6), 336.
2. Maghraby, Y. R., El-Shabasy, R. M., Ibrahim, A. H., & Azzazy, H. M. E. S. (2023). Enzyme

immobilization technologies and industrial applications. *ACS omega*, *8*(6), 5184-5196.

3. Perez-Velazquez, M., Maldonado-Othón, C. A., & González-Félix, M. L. (2024). Molecular weights and optimum temperature and pH for pepsin activity of three sciaenid finfish species from the Gulf of California. *Archives of Biological Sciences*, *76*(1), 83-90.
4. Ranganathan, P., & Raja, V. K. (2024). Maximizing Efficiency and Affordability with Ceramic Membranes for Enzyme Immobilization. *Chemical Engineering & Technology*, *47*(3), 552-560.
5. Dutt, K., & Meghwanshi, G. K. (2024). Advances in Fungal Enzymes and Their Applications. In *Applied Mycology for Agriculture and Foods* (pp. 383-419). Apple Academic Press.
6. Rodrigues, R. C., Berenguer-Murcia, Á., Carballares, D., Morellon-Sterling, R., & Fernandez-Lafuente, R. (2021). Stabilization of enzymes via immobilization: Multipoint covalent attachment and other stabilization strategies. *Biotechnology advances*, *52*, 107821.
7. Cavalcante, F. T., Cavalcante, A. L., de Sousa, I. G., Neto, F. S., & dos Santos, J. C. (2021). Current status and future perspectives of supports and protocols for enzyme immobilization. *Catalysts*, *11*(10), 1222.
8. Niu, Y., Wu, J., Kang, Y., Sun, P., Xiao, Z., & Zhao, D. (2023). Recent advances of magnetic chitosan hydrogel: Preparation, properties and applications. International Journal of Biological Macromolecules,125722.https://www.sciencedirect.com/science/article/pii/S0141813023026168.
9. Sharouf, H., & Saffour, Z. (2024). Synthesizing and using iron oxide nanoparticles as nanocomposite in cotton fabrics nanofinishing. *Baghdad Science Journal*, *21*(1), 00720072.https://bsj.uobaghdad.edu.iq/index.php/BSJ/article/view/7743
10. Al-Tameemi, A. I., Masarudin, M. J., Rahim, R. A., Timms, V., Neilan, B., & Isa, N. M. (2023). ANTIBACTERIAL PROPERTIES OF ZINC OXIDE NANOPARTICLES SYNTHESIZED BY THE SUPERNATANT OF WEISSELLA CONFUSA UPM22MT04. *Iraqi Journal of Agricultural Sciences*, *54*(5), 1209-1222. https://doi.org/10.36103/ijas.v54i5.1816.
11. Al-Shaabani, M. J. M., Al-Ethawi, A. M. T., & AL-Mathkhury, H. J. (2020). Eco-frienly synthesis of gold nanoparticles and study their effect with antibiotics against Acinetobacter baumannii. *Iraqi Journal of Agricultural Sciences*, *51*(4).https://doi.org/10.36103/ijas.v51i4.1099.
12. Alden, M. A., & Yaaqoob, L. A. (2022). Evaluation of the Biological Effect Synthesized Zinc Oxide Nanoparticles on Pseudomonas aeruginosa. *Iraqi Journal of Agricultural Sciences*, *53*(1), 27-37. https://doi.org/10.36103 /ijas.v53i1.1502.
13. Saeed, M. A., Ghafoor, D. A., Hamid, M. K., & Yas, R. M. (2020). Synthesis and characterization of gold nanoparticles by aluminum as a reducing agent. *Baghdad Science Journal*, *17*(1), 336-341. https://www.iasj.net /iasj/download/000a375a8a45a1d9.
14. Mustafa, H. J., & Al-Saadi, T. M. (2021). Effects of gum arabic-coated magnetite nanoparticles on the removal of Pb ions from aqueous solutions. *Iraqi Journal of Science*, 889-896. https://www.iasj.net/iasj/download/b92948e79cce3374.
15. Hasan Huseen, R., A Taha, A., & M Abdul Hussien, A. (2021). Cytotoxicity and antibacterial activities of coated and non-coated magnetic nanoparticles. Journal of Nanostructures, 11(4), 698-710.https://jns.kashanu.ac.ir/article_111552.html.
16. Varamini, M., Zamani, H., Hamedani, H., Namdari, S., & Rastegari, B. (2022). Immobilization of horseradish peroxidase on lysine-functionalized gum Arabic-coated Fe3O4 nanoparticles for cholesterol determination. Preparative Biochemistry & Biotechnology, 52(7), 737-747 .https://www.tandfonline.com/doi/abs/10.1080/10826068.2021.1992780.
17. Guisan, J. M. (2013). New opportunities for immobilization of enzymes. Immobilization of Enzymes and Cells: Third Edition, 1-13.https://link.springer.com/protocol/10.1007/978-1-62703-550-7_1.
18. Auda, J. M., & Khalifa, M. I. (2019). Cloning and expression of a lipase gene from Pseudomonas Aeruginosa into E. Coli. *Iraqi Journal of Agricultural Sciences*, *50*(3), 768-775. https://doi.org/10.36103/ijas.v50i3.693.
19. Jebur, H. A., & Auda, J. M. (2020). Evalution of antimicrobial activity of partial purified bacteriocin from local isolate of Bacillus licheniforims HJ2020 MT192715. 1. *Iraqi Journal of Agricultural Sciences*, *51*(6). https://doi.org/10.36103/ijas.v51i6.1191.
20. Usman, A., Mohammed, S., & Mamo, J. (2021). Production, optimization, and characterization of an acid protease from a filamentous fungus by solid-state fermentation. International journal of microbiology, 2021.https://www.hindawi.com/journals /ijmicro/2021/6685963/.
21. Adnan, M., Li, K., Xu, L., & Yan, Y. (2018). X-shaped ZIF-8 for immobilization rhizomucor

miehei lipase via encapsulation and its application toward biodiesel production. Catalysts, 8(3), 96.https://www.mdpi.com/2073-4344/8/3/96.

22. Shrestha, S., Wang, B., & Dutta, P. (2020). Nanoparticle processing: Understanding and controlling aggregation. *Advances in colloid and interface science*, *279*, 102162. https://www.sciencedirect.com/science/article/pii/S0001868619304816.
23. Birniwa, A. H., Mohammad, R. E. A., Ali, M., Rehman, M. F., Abdullahi, S. S. A., Eldin, S. M., ... & Jagaba, A. H. (2022). Synthesis of gum Arabic magnetic nanoparticles for adsorptive removal of ciprofloxacin: equilibrium, kinetic, thermodynamics studies, and optimization by response surface methodology. *Separations*, *9*(10), 322. https://doi.org/10.3390/separations9100322.
24. Calzoni, E., Cesaretti, A., Tacchi, S., Caponi, S., Pellegrino, R. M., Luzi, F., ... & Di Michele, A. (2021). Covalent immobilization of proteases on polylactic acid for proteins hydrolysis and waste biomass protein content valorization. Catalysts, 11(2), 167.https://www.mdpi.com/2073-4344/11/2/167.
25. Jeyapragasam, T., & Saraswathi, R. (2014). Electrochemical biosensing of carbofuran based on acetylcholinesterase immobilized onto iron oxide–chitosan nanocomposite. Sensors and Actuators B: Chemical, 191, 681-687. https://www.sciencedirect.com/science/article/pii/S0925400513012409.
26. Shakir, Z. S., Yaseen, S. K., & Dhaigham, A. A. R. (2024). Comparison of surface-enhanced Raman scattering in star-shaped and cubic-shaped colloidal silver nanoparticles. Baghdad Science Journal. https://doi.org/10.21123/bsj.2024.9152.
27. Bilal, M., Iqbal, H. M., Adil, S. F., Shaik, M. R., Abdelgawad, A., Hatshan, M. R., & Khan, M. (2022). Surface-coated magnetic nanostructured materials for robust bio-catalysis and biomedical applications-A review. *Journal of Advanced Research*, *38*, 157-177. https://www.sciencedirect.com/science/article/pii/S2090123221001946.
28. Su, K. Y., & Lee, W. L. (2020). Fourier transform infrared spectroscopy as a cancer screening and diagnostic tool: a review and prospects. *Cancers*, *12*(1), 115. https://www.mdpi.com/2072-6694/12/1/115.
29. Mansour, A. T., Alprol, A. E., Abualnaja, K. M., El-Beltagi, H. S., Ramadan, K. M., & Ashour, M. (2022). Dried brown seaweed's phytoremediation potential for methylene blue dye removal from aquatic environments. *Polymers*, *14*(7), 1375. https://www.mdpi.com/2073-4360/14/7/1375.
30. Vargues, F., Brion, M. A., Rosa da Costa, A. M., Moreira, J. A., & Ribau Teixeira, M. (2021). Development of a magnetic activated carbon adsorbent for the removal of common pharmaceuticals in wastewater treatment. *International Journal of Environmental Science and Technology*, *18*, 2805-2818. https://dx.doi.org/10.4314/cajost.v6i1.4.
31. Bakshi, J., Mehra, M., Grewal, S., Dhingra, D., & Kumari, S. (2022). Synthesis, characterization and evaluation of in vitro antimicrobial and anti-diabetic activity of berberine encapsulated in guar-acacia gum nanocomplexes. Journal of Bioactive and Compatible Polymers, 37(4), 233-251. https://doi.org/10.1177/08839115221106700.
32. Vimala, K., Kanny, K., Padma, Y., Velchuri, R., Ravi, G., Reddy, B. J., … & Vithal, M. (2018). Development of alginate-gum acacia-ag0 nanocomposites via green process for inactivation of foodborne bacteria and impact on shelf life of black grapes (vitis vinifera). Journal of Applied Polymer Science, 136(15). https://doi.org/10.1002/app.47331.
33. Ali, I. H., Bani-Fwaz, M. Z., El-Zahhar, A. A., Marzouki, R., Jemmali, M., & Ebraheem, S. M. (2021). Gum Arabic-magnetite nanocomposite as an eco-friendly adsorbent for removal of lead (II) ions from aqueous solutions: equilibrium, kinetic and thermodynamic studies. *Separations*, *8*(11), 224. https://www.mdpi.com/2297-8739/8/11/224.
34. Baird, G., Farrell, C., Cheung, J., Semple, A., Blue, J., & Ahl, P. L. (2020). FTIR spectroscopy detects intermolecular β-sheet formation above the high temperature T m for two monoclonal antibodies. *The Protein Journal*, *39*, 318-327. https://link.springer.com/article/10.1007/s10930-020-09907-y.
35. Mirza, S., Jolly, R., Zia, I., Saad Umar, M., Owais, M., & Shakir, M. (2020). Bioactive gum Arabic/κ-carrageenan-incorporated nano-hydroxyapatite nanocomposites and their relative biological functionalities in bone tissue engineering. *ACS omega*, *5*(20), 11279-11290. https://pubs.acs.org/doi/abs/10.1021/acsomega.9b03761.
36. Mohammadi, Z. B., Zhang, F., Kharazmi, M. S., & Jafari, S. M. (2023). Nano-biocatalysts for food applications; immobilized enzymes within different nanostructures. Critical reviews in food science and nutrition, 63(32), 11351-11369. https://www.tandfonline.com/doi/abs/10.1080/10408398.2022.2092719.
37. Liu, D. M., & Dong, C. (2020). Recent advances in nano-carrier immobilized enzymes and their applications. *Process Biochemistry*, *92*, 464-475.

https://www.sciencedirect.com/science/article/pii/S1359511319315004.

38. Farooq, S., Ahmad, M. I., Ali, U., & Zhang, H. (2024). Fabrication of curcumin-loaded oleogels using camellia oil bodies and gum arabic/chitosan coatings for controlled release applications. *International Journal of Biological Macromolecules*, *254*, 127758. https://www.sciencedirect.com/science/article/pii/S0141813023046573.
39. Oke, M. A., Ojo, S. A., Fasiku, S. A., & Adebayo, E. A. (2023). Nanotechnology and enzyme immobilization: a review. *Nanotechnology*, *34*(38), 385101. https://iopscience.iop.org/article/10.1088/1361-6528/acda35/meta.
40. Behshad, Y., Pazhang, M., Najavand, S., & Sabzi, M. (2023). Enhancing enzyme stability and functionality: covalent immobilization of trypsin on magnetic gum arabic modified Fe3O4 nanoparticles. *Applied Biochemistry and Biotechnology*, 1-18. https://link.springer.com/article/10.1007/s12010-023-04830-1.
41. Nayeri, M. D., Nikkhah, H., Zilouei, H., & Bazarganipour, M. (2023). Immobilization of cellulase on graphene oxide coated with NiFe2O4 and Fe3O4 for hydrolysis of rice straw. Cellulose, 30(9), 5549-5571. https://link.springer.com/article/10.1007/s10570-023-05207-7.
42. Kumar, A., Mukhia, S., Kumar, N., Acharya, V., Kumar, S., & Kumar, R. (2020). A broad temperature active lipase purified from a psychrotrophic bacterium of sikkim himalaya with potential application in detergent formulation. *Frontiers in bioengineering and biotechnology*, *8*, 642. https://www.frontiersin.org/articles/10.3389/fbioe.2020.00642/full.
43. Taheri-Kafrani, A., Kharazmi, S., Nasrollahzadeh, M., Soozanipour, A., Ejeian, F., Etedali, P., ... & Varma, R. S. (2021). Recent developments in enzyme immobilization technology for high-throughput processing in food industries. *Critical Reviews in Food Science and Nutrition*, *61*(19), 3160-3196. https://www.tandfonline.com/doi/abs/10.1080/10408398.2020.1793726.
44. Anwar, A., Imran, M., & Iqbal, H. M. (2023). Smart chemistry and applied perceptions of enzyme-coupled nano-engineered assemblies to meet future biocatalytic challenges. *Coordination Chemistry Reviews*, *493*, 215329. https://www.sciencedirect.com/science/article/pii/S0010854523003181.
45. Mehdi, W. A., Mehde, A. A., Özacar, M., & Özacar, Z. (2018). Characterization and immobilization of protease and lipase on chitin-starch material as a novel matrix. International journal of biological macromolecules, 117, 947-958.https://www.sciencedirect.com/science/article/pii/S0141813018311048.